NANO LETTERS

Letter

pubs.acs.org/NanoLett

Long Spin Relaxation Times in Wafer Scale Epitaxial Graphene on SiC(0001)

Thomas Maassen,*[,†] J. Jasper van den Berg,[†] Natasja IJbema,[†] Felix Fromm,[‡] Thomas Seyller,[‡] Rositza Yakimova,[§] and Bart J. van Wees[†]

[†]Physics of Nanodevices, Zernike Institute for Advanced Materials, University of Groningen, Nijenborgh 4, 9747 AG Groningen, The Netherlands

[‡]Lehrstuhl für Technische Physik, Universität Erlangen-Nürnberg, Erwin-Rommel-Strasse 1, 91058 Erlangen, Germany

[§]Department of Physics, Chemistry and Biology (IFM), Linköping University, S-581 83 Linköping, Sweden

ABSTRACT: We developed an easy, upscalable process to prepare lateral spin-valve devices on epitaxially grown monolayer graphene on SiC(0001) and perform nonlocal spin transport measurements. We observe the longest spin relaxation times τ_S in monolayer graphene, while the spin diffusion coefficient D_S is strongly reduced compared to typical results on exfoliated graphene. The increase of τ_S is probably related to the changed substrate, while the cause for the small value of D_S remains an open question.

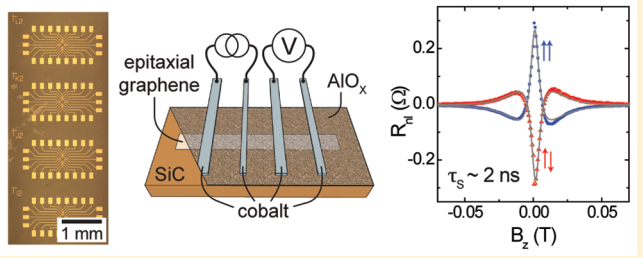

KEYWORDS: *Spin transport, Hanle precession, graphene, epitaxial growth*

Spin transport in graphene draws great attention because of the observation of spin relaxation lengths of $\lambda_S = 2\ \mu$m with spin relaxation times in the order of $\tau_S = 150$ ps at room temperature (RT) in mechanical exfoliated single layer graphene (eSLG).[1] Recent experiments show an increase of τ_S to $\tau_S \approx 0.5$ ns in eSLG at RT[2,3] and $\tau_S \approx 1$ ns at $T = 4$ K.[3] Measurements on bilayer graphene (BLG) show even higher spin relaxation times of up to a few nanoseconds at low temperature.[3,4] At the same time, a study on few-layer graphene (FLG) showed an enhancement of τ_S with increasing number of layers, which is attributed to the screening of external scattering potentials.[5]

While most spin transport measurements were performed on exfoliated graphene, a first publication by Avsar et al.[6] showed measurements on graphene, grown by chemical vapor deposition (CVD) on copper foil. This publication marked the first step toward large scale production of spin transport devices, which showed similar spin transport properties compared to exfoliated graphene. The disadvantage of the graphene growth on metal substrates is, however, that one is forced to transfer the material to an insulating substrate to be able to perform transport measurements.

Therefore, it is useful to think about an alternative, for example, epitaxially grown graphene on semi-insulating SiC.[7,8] This letter is the first report of spin transport in this material and therefore the first report of spin transport in graphene on a different substrate than SiO_2. We present lateral nonlocal spin-valve and spin-precession measurements on graphene strips prepared from monolayer epitaxial graphene (MLEG) grown on the Si-face of a semi-insulating SiC substrate (SiC(0001)) by sublimation of Si in Ar atmosphere.[8−10]

The 4H-SiC wafers[11] are heated to 2000 °C in an ambient argon pressure of 1 atm as described in refs 8 and 9, leading to the growth of the so-called buffer layer that is predominately (>80%) covered with MLEG with some areas uncovered or covered with double layer graphene. The measurements were performed on MLEG[12] and with the help of Hall measurements on similar samples we estimate an electron doping with a charge carrier density of $n \approx 3 \times 10^{12}$ cm^{-2} and a charge carrier mobility of $\mu \approx 1900$ cm^2 V^{-1} s^{-1} at RT.

Figure 1a shows an about 7 × 5 mm^2 big part of a SiC wafer covered with MLEG, prepared with a pattern of Ti/Au structures that form a periodic pattern of bondpads with leads to central 100 × 100 μm^2 areas for further device preparation. These structures are prepared in an optical lithography step, using a deep-UV mask aligner with a double resist layer (LOR-3A/ZEP-520A, from MicroChem/ZEON Corporation). After development, the wafer is etched with oxygen plasma at 40 W for 20 s, before depositing a Ti/Au (5 nm/35 nm) double layer using e-beam evaporation followed by lift-off in PRS-3000 (from J.T. Baker). The etching step is necessary to enable the adhesion of the Ti/Au contacts on the substrate. To prepare the central device regions (Figure 1b), two MLEG strips per area are defined, using e-beam lithography (EBL) on a negative resist (ma-N 2400, from microresist technology GmbH) and the uncovered MLEG is etched in a second oxygen plasma etching step. After this, the wafer is annealed for two hours in Ar(95%)/H$_2$(5%)

Received: December 2, 2011
Revised: January 23, 2012
Published: February 10, 2012

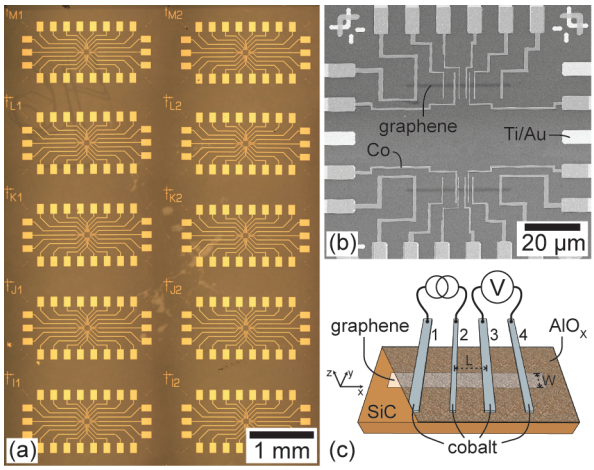

Figure 1. (a) Optical microscope picture of a SiC wafer prepared with Ti/Au bondpads and leads to central 100 × 100 μm^2 areas for further device preparation. Each of these patterns has a unique label for further production steps and measurements. The changes in the background color are due to scratches and resist residues on the backside of the transparent SiC wafer. (b) SEM picture of one of the central device areas with two spin valve devices, connected with Co electrodes to the Ti/Au leads. (c) Sketch of an MLEG spin valve device with four Co contacts. The wafer including the MLEG strip is covered with AlO_x before the Co contacts are deposited.

environment at 350 °C to remove resist residues. To avoid the conductivity mismatch,[13−15] the wafer is covered with an approximately 1 nm thick AlO_x layer by evaporating 0.4 nm aluminum at a base pressure of $p < 1 \times 10^{-6}$ mbar, oxidation in situ in O_2 atmosphere at a base pressure of $p > 3 \times 10^{-5}$ mbar for 15 min and repeating the step a second time. Finally, in a standard PMMA resist-based EBL step, the 45 nm thick Co electrodes are formed (Figure 1b) connecting the Ti/Au leads with the two graphene strips, before the bondpads are contacted using wire bonding. By preparing the wafer with an optical step and using EBL only on the small central areas, we developed a fast and easy process to prepare a full wafer with (spin) transport devices. This process can also be used for different types of large area graphene on nonconducting substrates.

As the resolution of the ma-N resist is limited to about 50 nm, we developed a second process, replacing the ma-N resist step with a PMMA step. This enables a higher resolution but in return requires an additional step to remove the graphene outside the 100 × 100 μm^2 areas to disconnect the Ti/Au leads. This method was implemented for two devices, using an additional optical lithography step, where we cover the central device areas, while the exposed graphene is removed with oxygen plasma.

The presented measurements are performed on a $W = 0.7$ μm wide MLEG strip in vacuum at a base pressure of about 1×10^{-6} mbar using low-frequency lock-in technique and AC currents between 1 and 10 μA. The measurements have been confirmed with consistent results, that have been obtained on several spin-valve areas on two other devices with $W = 1$ μm.

The typical nonlocal geometry is presented in Figure 1(c). A spin polarized current I is sent from contact 2 to contact 1, generating a spin accumulation at contact 2 that diffuses in positive and negative x-direction. The AlO_x barrier separates the MLEG from the Co contacts and avoids reabsorption of the injected spins in the higher conducting cobalt.[14] The exponential decaying spin accumulation generates a nonlocal voltage V_{nl} between the spin sensitive contacts 3 and 4, which can be measured as a function of the magnetic field. In a spin-valve measurement, the magnetic field B_y, aligned with the contacts, is first used to bring the magnetization of the electrodes into a parallel (P) configuration and is then ramped in the opposite direction. When the magnetization of one of the electrodes is switched, the measured voltage shows abrupt changes. The magnetic switching fields of the contacts are different due to different coercive fields that are achieved by different width of the contacts.[1,14]

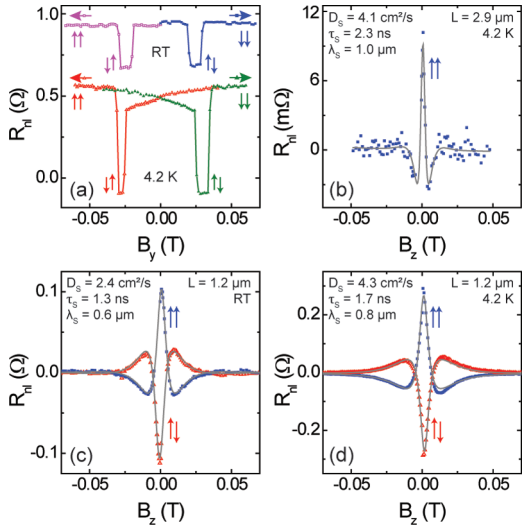

Figure 2. Nonlocal spin transport measurements. (a) Spin valve measurements on a device with $L = 1.2$ μm inner contact distance at RT (purple and blue) and 4.2 K (red and green). The sweep directions of the magnetic field are indicated by the horizontal arrows, the relative orientation of the Co contacts is illustrated by the pairs of vertical arrows. (b−d) Hanle precession measurement for parallel (↑↑, blue boxes) and antiparallel alignment (↑↓, red open triangles) of the inner electrodes for (b) $L = 2.9$ μm at 4.2 K, (c) $L = 1.2$ μm at RT, and (d) $L = 1.2$ μm at 4.2 K. The fits to the solutions of the Bloch equation are plotted in gray. The background resistance, which is visible in (a), is subtracted in the Hanle precession measurements (b−d).

Figure 2a shows two spin-valve measurements, one at RT and one at 4.2 K. V_{nl}, normalized to the nonlocal resistance $R_{nl} = V_{nl}/I$, is plotted as a function of the magnetic field. The upper measurement has been obtained at RT. After saturating the magnetization of the contacts at $B_x \approx -450$ mT no change of R_{nl} is observed, before B_y crosses $B_y = 0$ (not shown). Then at $B_y = 18$ mT a switch in R_{nl} by 250 mΩ is observed that can be attributed to the antiparallel alignment (AP) of injector and detector before it switches back to P and the initial R_{nl} value at $B_y = 30$ mT. On the basis of only two visible switches, it can be concluded that the outer contacts (contact 1 and 4 in Figure 1c) are giving no significant contribution to the signal.[1] The relatively small amplitude of the signal of $2R_{nl} = 250$ mΩ is not necessarily related to spin relaxation in the graphene strip but is here related to the relatively low polarization of the contact interface. Also, the contact interface is described by the R parameter, which is in our measurements $R = WR_C/R_{sq} \geq 2.1$ μm with a contact resistance of $R_C \geq 3.3$ kΩ, a square resistance of the MLEG of $R_{sq} = 1.1$ kΩ and $W = 0.7$ μm.[14,16]

dx.doi.org/10.1021/nl2042497 | Nano Lett. 2012, 12, 1498−1502

Therefore the contacts are almost noninvasive but can still slightly influence the spin transport measurements.[14,15]

The spin valve measurement, performed at T = 4.2 K, shows similar behavior. The main differences are that the amplitude is approximately doubled and the switching fields are slightly increased due to a change in the coercive fields with decreased temperature. Additional, R_{nl} shows a gradual decrease in its value before the contacts switch to AP. This is probably due to a slight misalignment of the magnetic field and the electrodes. The changed background resistance is mainly influenced by heat related effects[17,18] and can therefore change with temperature.

To analyze the spin transport properties, we perform Hanle spin precession measurements.[13] For this purpose, the magnetic field is aligned in z-direction. The resulting spin dynamics are described with the one-dimensional Bloch equation for the spin accumulation $\vec{\mu}_s$[13]

$$D_S\nabla^2\vec{\mu}_S - \frac{\vec{\mu}_S}{\tau_S} + \vec{\omega}_0 \times \vec{\mu}_S = \vec{0} \quad (1)$$

The first term on the left-hand side describes the spin-diffusion represented by the spin-diffusion coefficient D_S, and the second term describes the spin relaxation with the spin relaxation time τ_S. The third term describes the precession with the Larmor frequency $\vec{\omega}_0 = g\mu_B/\hbar\vec{B}$, where $g \approx 2$ is the effective Landé factor and μ_B is the Bohr magneton.

The Hanle precession measurements in Figure 2b–d can be fitted with the solutions of the Bloch equation (eq 1), yielding the spin transport quantities D_S and τ_S. A summary of the fitting results is shown in Table 1. Figure 2b shows Hanle precession measurements, performed on a distance of L = 2.9 μm at 4.2 K. The fit gives D_S = 4.06 ± 0.05 cm^2/s and τ_S = 2.34 ± 0.28 ns, resulting in $\lambda_S = (D_S\tau_S)^{1/2}$ = 0.98 ± 0.06 μm.

Table 1. Results of the Fits to the Measurements in Figure 2b–d

L (μm)	2.9	1.2	1.2
T (K)	4.2	4.2	293
D_S (cm^2/s)	4.06 ± 0.05	4.26 ± 0.06	2.38 ± 0.03
τ_S (ns)	2.34 ± 0.28	1.66 ± 0.02	1.34 ± 0.02
λ_S (μm)	0.98 ± 0.06	0.84 ± 0.01	0.56 ± 0.01
R_{nl} (mΩ)	9.2 ± 0.4	275.7 ± 2.2	102.9 ± 0.7

We would like to note that this value for τ_S is the longest reported spin relaxation time on monolayer graphene. And as the contacts are to some extent invasive, we can expect even higher values for τ_S, because a part of the injected spins relax at the contact interface. The effect of the contacts becomes apparent if one compares the fits of the measurement at L = 2.9 μm and L = 1.2 μm at 4.2 K (Figure 2b,d). For the measurement at L = 1.2 μm, we get τ_S = 1.66 ± 0.02 ns, which is around 70% of the τ_S obtained from the L = 2.9 μm measurement. This is because the contact induced relaxation is more influential, the shorter the distance the spins diffuse in the graphene strip between the contacts.[15] With invasive contacts, the shorter measurement distance also leads to a slight increase in the measured D_S.[15] Also this is observed, comparing the L = 1.2 μm to the L = 2.9 μm precession measurement at 4.2 K.

When measuring at RT (Figure 2c) we observe a reduction of D_S by more than 40% and τ_S is decreased by about 20%. Therefore we get λ_S = 0.56 ± 0.01 μm, which is one-third smaller than λ_S at 4.2 K (see Table 1). We also observe slightly higher values for τ_S of up to ∼1.5 ns (not shown). Figure 3 shows a more detailed temperature dependence of τ_S, D_S, λ_S, and the nonlocal signal amplitude R_{nl} between 4.2 K and RT. All four parameters show a decline over the whole temperature range. While D_S and λ_S are monotonically decreasing by 40 and 30%, respectively, the value of τ_S and R_{nl} drops by 20% and a factor of 3, respectively. The decrease of all four values can be related to electron–phonon scattering.[13,19] τ_S and R_{nl} are approximately constant below 100 K, which could be related to the fact that the phonons are frozen out below that temperature. Given the relatively low mobility of the graphene, the temperature dependence could also be dominated by Coulomb scattering on trapped charges in the SiC substrate which shows a strong temperature dependence as described by Farmer et al.[20]

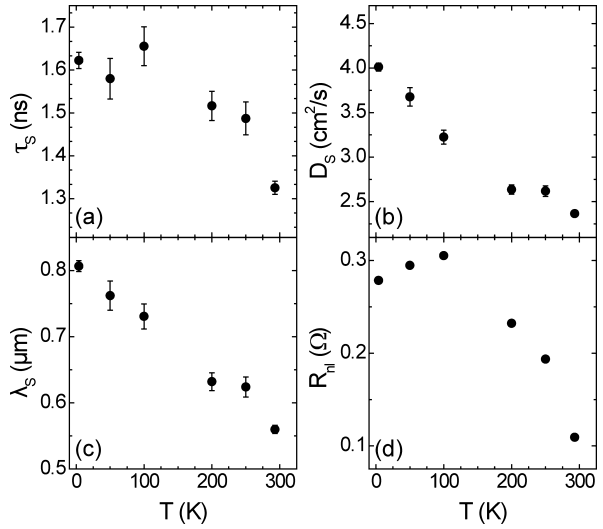

Figure 3. Temperature dependence of (a) the spin relaxation time, (b) the spin diffusion coefficient, (c) the spin relaxation length, and (d) the nonlocal signal for the sample with L = 1.2 μm. If available, several fitting results at the same temperature were averaged.

Our typical values for eSLG on SiO_2 at RT are in the case of D_S about a factor of 80× bigger, however the measurements on MLEG strips show an increase of τ_S by about a factor of 10. This still leads to a ∼70% lower value for λ_S.[14,21] The increase in τ_S in MLEG compared to eSLG can be attributed to the changed substrate. While SiO_2 has an electrical inhomogeneous surface potential leading to electron–hole puddles[22] and limiting effects for spin transport in graphene,[23] the SiC crystal and the buffer layer are far more homogeneous and reduce therefore scattering. We would like to note that in our measurements on exfoliated graphene the spin transport properties are only weakly influenced by the temperature[1,5] whereas we here see an improvement at low temperatures.

Although τ_S is improved, we do not know the origin for the reduced values of D_S. We obtain the diffusion coefficient D_S from Hanle spin precession measurements. To verify if the value for D_S is correct, we compare it to the diffusion coefficient D_C acquired from charge transport measurements on the same area. D_C is calculated using the Einstein relation $D_C = (R_{sq}e^2\nu(E_F))^{-1}$, where e is the electron charge and ν is the density of states (DOS). The band structure for MLEG on SiC(0001) is the same as for eSLG.[7] Therefore, we can assume the same DOS as for eSLG, $\nu(E) = g_v g_s 2\pi|E|/(h^2 v_F^2)$ with the

dx.doi.org/10.1021/nl2042497 | Nano Lett. 2012, 12, 1498–1502

two-fold valley ($g_v = 2$) and spin ($g_s = 2$) degeneracies and the Fermi velocity $v_F \approx 10^6$ ms^{-1}. With n estimated by Hall measurements on similar devices and $n(E_F) = \int_0^{E_F} \nu(E)dE$ we can calculate the Fermi energy E_F and receive $\nu(E_F)$. With $n \approx 3 \times 10^{12}$ cm^{-2} and $R_{sq} = 1.1$ kΩ, we get $D_C \approx 190$ cm^2/s, which is similar to typical values obtained in eSLG.[21] This is not surprising, because the charge carrier mobility in our samples is with $\mu = (R_{sq}en)^{-1} \approx 1900$ cm^2 V^{-1} s^{-1} reasonably close to the mobility of our eSLG devices.[21]

But this value of D_C means that we observe a difference between the charge diffusion coefficient D_C and D_S of a factor 45 to 80 (compare Table 1) in contrast to $D_C \approx D_S$ in eSLG.[21] D_S and D_C can in principle be different as observed by Weber et al.[24] in a two-dimensional electron gas. Here the effect is attributed to electron−electron interactions but was significantly smaller than in our results. In FLG, a slight difference of ∼20% between the two coefficients is found,[5] but that difference is not comparable to the observation here.

We therefore do not expect a difference between the diffusion coefficient obtained from charge transport measurements and from Hanle precession measurements. While we cannot explain the observed difference, yet, we can exclude some possible explanations for it.

We do not expect the D_C value to be incorrect as the observed charge transport is comparable to eSLG. One aspect though, that could result in a wrong D_C value, are extra current paths next to the MLEG strip which would result in a change of the observed R_{sq}. We can exclude this by carefully controlling the etched structures with a scanning electron microscope (SEM) and by confirming that contacts of different MLEG strips show no conduction between each other.

n was determined by Hall measurements on similar samples but not on the spin transport samples themselves, therefore there could be an error in the value for n that would lead to an incorrect value for the DOS. The highest values for n, measured on MLEG samples on SiC(0001), under the described growth conditions, are around $n \approx 1 \times 10^{13}$ cm^{-2}, which leads to $D_C \approx 100$ cm^2/s. This changes D_C by less than a factor of 2 and smaller values for n would only increase the calculated value for D_C. Hence, also this aspect does not explain the difference between D_S and D_C.

Another possibility would be a wrongly assumed DOS. Though, to result in values for D_C similar to D_S we would need a DOS as high as ∼50 times the DOS of BLG. But we can be sure that we do not have such a DOS in our system because similar material to that used in our studies shows the typical quantum Hall effect (QHE) of eSLG.[9,25]

Since we do not find any explanation for the difference between D_C and D_S in the way D_C is determined, let us have a look at D_S. D_S is obtained by the fit of the Hanle precession data in the same way as in earlier experiments.[1,5,14,21] Therefore the fitting procedure cannot explain the difference in the values, as the result for eSLG, $D_C \approx D_S$, is based on fits to measurements on eSLG using the same procedure. Next to that, we can confirm the value for D_S in a different way. As mentioned before, the small value for D_S leads to a relatively small value for λ_S. The order of magnitude of this value can be confirmed by comparing the change of R_{nl} with L. By fitting an exponential decay[13] to the two R_{nl} values versus L for the data obtained at 4.2 K (see Table 1, fit not shown), we receive $\lambda_S \approx 0.5$ μm, which is in agreement with the order of magnitude of λ_S obtained from our fitted τ_S and D_S.[26] With $D_S = D_C \approx 200$ cm^2 s^{-1} and $\tau_S \approx 2$ ns, we would receive a λ_S of 1 order of magnitude larger.

While λ_S is confirmed, there is still the possibility that the prefactor of the precession term in the Bloch equation (eq 1) is wrong, which would affect linearly the determination of D_S and $1/\tau_S$. This would be the case, if the effective Landé factor g is changed in our system. But the reduction of g by a factor of ∼50 is needed to result in our measured D_S. This is unlikely, also since $g \approx 2$ was confirmed for epitaxial multilayer graphene on the C-face of SiC.[27]

A change of D_S can only be caused by the substrate as we expect the graphene to be comparable to eSLG[7] and growth related defects like grain boundaries do not show a strong effect on D_S and τ_S for CVD grown single layer graphene on SiO_2.[6] One of the substrate related effects could be inhomogeneities of the graphene thickness and doping at terrace step edges[7] and scattering potentials resulting from that. However, this is relatively unlikely since step edges are not resulting in a discontinuity of the graphene layer.[7] On the other hand, the out-of-plane electric field between the bulk SiC and the buffer layer[7] could have an effect on the spin transport.

Another possible reason for the change in the spin transport properties could be related to the buffer layer. Its topology is graphene-like, though a part of the C atoms is covalently bonded to the underlying Si atoms. Therefore, the layer is electrically inactive and only weakly interacts with graphene layers on top.[28] The buffer layer does not seem to affect charge transport, at least not the measured resistance or the QHE,[7] although it influences the temperature dependence of the charge carrier mobility.[29] However, localized states in the buffer layer could act as hopping sites for electron spins and could influence the spin relaxation and the spin diffusion. By spins hopping into these states and back, D_S could be reduced without affecting R_{sq} and therefore the determined D_C (as we do not include these extra states in the DOS). This kind of localized states could also originate from Al clusters in the AlO_x barrier. When depositing the barrier, some of the Al atoms could cluster and if their size exceeds some certain limit, part of the Al could stay nonoxidized. Those clusters would have a high DOS compared to the MLEG and could therefore have a relatively strong influence on the diffusion. This effect is unlikely, as we do not see it for eSLG on SiO_2 but the less rough surface of MLEG on SiC and the resulting difference in the growth mechanism could result in this clustering. Here it would be interesting to produce samples with the AlO_x barrier only locally below the contacts as discussed in ref 14 to compare the spin transport properties with the here reported results.

One other effect that could affect the measurements is the influence that the Ar(95%)/H_2(5%) cleaning at 350 °C could have on the buffer layer. Speck et al.[29] discuss the intercalation of hydrogen in epitaxial graphene on SiC that leads to the transformation of the buffer layer into an extra graphene layer. Though the discussed experiment uses about 1 bar pure hydrogen at 550 °C for 75 min, our cleaning step could partly intercalate hydrogen below the graphene layer and this could lead to extra transport channels and influence the transport measurements.

None of these considerations above led to a conclusive explanation of the observed difference between the diffusion coefficients obtained from charge and spin transport measurements. Therefore, we have to wait for further measurements to determine if the difference is based on the way those values are

dx.doi.org/10.1021/nl2042497 | Nano Lett. 2012, 12, 1498−1502

obtained or if there is a difference between charge and spin diffusion in MLEG on SiC(0001). The effect of the buffer layer can be addressed by measuring spin transport on quasi freestanding MLEG on SiC[29] and general substrate related effects can be examined by transferring MLEG to SiO_2.[30]

In summary, we present a fast and easy process to prepare (spin) transport devices on wafer scale graphene by the example of MLEG. With this technique, we produced lateral spin-valve devices on MLEG and performed spin-valve and Hanle spin precession measurements between T = 4.2 K and RT. In the Hanle measurements, we observe exceptionally high values for τ_S of up to τ_S = 2.3 ns and very small values for D_S of $D_S < 5$ cm^2/s, resulting in a reduction of λ_S by a factor of 2 to 3 compared to eSLG. We observe a significant difference between the diffusion coefficient obtained from charge and spin transport measurements, which we discuss but cannot explain, yet. Finally, we present the temperature dependence of the spin transport and show a decrease for τ_S, D_S, λ_S, and R_{nl} with increasing temperature, that can be linked to electron−phonon scattering or Coulomb scattering on trapped charges in the SiC substrate.

AUTHOR INFORMATION

Corresponding Author

*E-mail: t.maassen@rug.nl.

Notes

The authors declare no competing financial interest.

ACKNOWLEDGMENTS

We would like to acknowledge P. J. Zomer, H. M. de Roosz, B. Wolfs, and J. G. Holstein for technical support and Sergey Kubatkin for helpful discussions. The research leading to these results has received funding from NanoNed, the Zernike Institute for Advanced Materials, the Foundation for Fundamental Research on Matter (FOM), the Deutsche Forschungsgemeinschaft and the European Union Seventh Framework Programme (FP7/2007-2013) under grant agreement "ConceptGraphene" Number 257829.

REFERENCES

(1) Tombros, N.; Józsa, C.; Popinciuc, M.; Jonkman, H. T.; van Wees, B. J. *Nature* **2007**, *448*, 571−574.

(2) Han, W.; Pi, K.; McCreary, K. M.; Li, Y.; Wong, J. J. I.; Swartz, A.; Kawakami, R. K. *Phys. Rev. Lett.* **2010**, *105*, 167202.

(3) Han, W.; Kawakami, R. K. *Phys. Rev. Lett.* **2011**, *107*, 047207.

(4) Yang, T.-Y.; Balakrishnan, J.; Volmer, F.; Avsar, A.; Jaiswal, M.; Samm, J.; Ali, S. R.; Pachoud, A.; Zeng, M.; Popinciuc, M.; Güntherodt, G.; Beschoten, B.; Özyilmaz, B. *Phys. Rev. Lett.* **2011**, *107*, 047206.

(5) Maassen, T.; Dejene, F. K.; Guimarães, M. H. D.; Józsa, C.; van Wees, B. J. *Phys. Rev. B* **2011**, *83*, 115410.

(6) Avsar, A.; Yang, T.-Y.; Bae, S.; Balakrishnan, J.; Volmer, F.; Jaiswal, M.; Yi, Z.; Ali, S. R.; Güntherodt, G.; Hong, B. H.; Beschoten, B.; Özyilmaz, B. *Nano Lett.* **2011**, *11*, 2363−2368.

(7) First, P. N.; de Heer, W. A.; Seyller, T.; Berger, C.; Stroscio, J. A.; Moon, J.-S. *MRS Bull.* **2010**, *35*, 296−305.

(8) Virojanadara, C.; Syväjarvi, M.; Yakimova, R.; Johansson, L. I.; Zakharov, A. A.; Balasubramanian, T. *Phys. Rev. B* **2008**, *78*, 245403.

(9) Tzalenchuk, A.; Lara-Avila, S.; Kalaboukhov, A.; Paolillo, S.; Syväjärvi, M.; Yakimova, R.; Kazakova, O.; Janssen, T. J. B. M.; Fal'ko, V.; Kubatkin, S. *Nat. Nanotechnol.* **2010**, *5*, 186−189.

(10) Emtsev, K. V.; Bostwick, A.; Horn, K.; Jobst, J.; Kellogg, G. L.; Ley, L.; McChesney, J. L.; Ohta, T.; Reshanov, S. A.; Rohrl, J.; Rotenberg, E.; Schmid, A. K.; Waldmann, D.; Weber, H. B.; Seyller, T. *Nat. Mat.* **2009**, *8*, 203−207.

(11) Shaffer, P. T. B. *Acta Crystallogr.* **1969**, *B25*, 477.

(12) The confirmation of the thickness to be MLEG is achieved by measuring R_{sq}.

(13) Fabian, J.; Matos-Abiague, A.; Ertler, C.; Stano, P.; Zutic, I. *Acta Phys. Slov.* **2007**, *57*, 565−907.

(14) Popinciuc, M.; Józsa, C.; Zomer, P. J.; Tombros, N.; Veligura, A.; Jonkman, H. T.; van Wees, B. J. *Phys. Rev. B* **2009**, *80*, 214427.

(15) Maassen, T.; Huisman, E. H.; van den Berg, J. J.; van Wees, B. J. in preparation.

(16) Both R_C and R_{sq} show only weak temperature dependence, therefore also R is not affected by T.

(17) Vera-Marun, I. J.; Ranjan, V.; van Wees, B. J. *J. Nat. Phys.* **2012**, DOI: 10.1038/nphys2219.

(18) Bakker, F. L.; Slachter, A.; Adam, J.-P.; van Wees, B. J. *Phys. Rev. Lett.* **2010**, *105*, 136601.

(19) Tanabe, S.; Sekine, Y.; Kageshima, H.; Nagase, M.; Hibino, H. *Phys. Rev. B* **2011**, *84*, 115458.

(20) Farmer, D. B.; Perebeinos, V.; Lin, Y.-M.; Dimitrakopoulos, C.; Avouris, P. *Phys. Rev. B* **2011**, *84*, 205417.

(21) Józsa, C.; Maassen, T.; Popinciuc, M.; Zomer, P. J.; Veligura, A.; Jonkman, H. T.; van Wees, B. J. *Phys. Rev. B* **2009**, *80*, 241403.

(22) Martin, J.; Akerman, N.; Ulbricht, G.; Lohmann, T.; Smet, J. H.; von Klitzing, K.; Yacoby, A. *Nat. Phys.* **2008**, *4*, 144−148.

(23) Ertler, C.; Konschuh, S.; Gmitra, M.; Fabian, J. *Phys. Rev. B* **2009**, *80*, 041405.

(24) Weber, C. P.; Gedik, N.; Moore, J. E.; Orenstein, J.; Stephens, J.; Awschalom, D. D. *Nature* **2005**, *437*, 1330−1333.

(25) Jobst, J.; Waldmann, D.; Speck, F.; Hirner, R.; Maude, D. K.; Seyller, T.; Weber, H. B. *Phys. Rev. B* **2010**, *81*, 195434.

(26) As the polarization of the contact, and therefore the induced spin accumulation, can vary significantly between different contacts, this analysis is not conclusive but allows a rough estimate of the order of magnitude of λ_S. The same analysis has been performed for the other two devices and has led to the same result.

(27) Song, Y. J.; Otte, A. F.; Kuk, Y.; Hu, Y.; Torrance, D. B.; First, P. N.; de Heer, W. A.; Min, H.; Adam, S.; Stiles, M. D.; MacDonald, A. H.; Stroscio, J. A. *Nature* **2010**, *467*, 185−189.

(28) Emtsev, K. V.; Speck, F.; Seyller, T.; Ley, L.; Riley, J. D. *Phys. Rev. B* **2008**, *77*, 155303.

(29) Speck, F.; Jobst, J.; Fromm, F.; Ostler, M.; Waldmann, D.; Hundhausen, M.; Weber, H. B.; Seyller, T. *Appl. Phys. Lett.* **2011**, *99*, 122106.

(30) Lee, D. S.; Riedl, C.; Krauss, B.; von Klitzing, K.; Starke, U.; Smet, J. H. *Nano Lett.* **2008**, *8*, 4320−4325.